Structural and Functional Characterization of Potent Antithrombotic Oligonucleotides Possessing Both Quadruplex and Duplex Motifs

Román F. Macaya,* Janet A. Waldron, Bruce A. Beutel, Hetian Gao, Michael E. Joesten, Meihua Yang, Rina Patel, Arthur H. Bertelsen, and Alan F. Cook

PharmaGenics, Inc., 4 Pearl Court, Allendale, New Jersey 07401

Received November 1, 1994; Revised Manuscript Received January 23, 1995[⊗]

ABSTRACT: We report the results of a selection for single-stranded DNA oligonucleotide ligands to the serine protease thrombin using recently developed methods. This selection yielded a family of DNA sequences that conform to a consensus structure comprised of a unimolecular quadruplex motif and complementary flanking sequences capable of forming an additional Watson−Crick duplex motif. This novel quadruplex/duplex structure was not reported in a previous selection for DNA molecules which bind to thrombin [Bock *et al.* (1992) *Nature 355*, 564−566]. All quadruplex/duplex molecules tested bound to thrombin with higher affinity than quadruplex structures lacking the duplex structure. However, binding affinities did not always correlate with inhibitory potency since some molecules with high affinity were not potent inhibitors *in vitro*. ^{1}H NMR spectroscopy studies demonstrated that the complementarity of bases in the duplex portion of a selected sequence allows it to form multimolecular structures. Constraining these molecules to the unimolecular quadruplex/duplex structure by bridging the 5′ and 3′ ends of the duplex motif with either triethylene glycol or disulfide bonds improved their thrombin inhibitory activity. All bridged quadruplex/duplex molecules were more potent inhibitors than molecules with only a quadruplex motif. Bridging the ends of these structures not only increased thrombin inhibition but also improved resistance to nucleases in serum more than 40-fold over the unbridged quadruplex. In addition, we have found that both the length and sequence of the duplex motif are important for inhibition.

Methods for the selection of nucleic acid ligands have been used to identify oligonucleotides with high affinity for proteins (Oliphant *et al.*, 1989; Kinzler & Vogelstein, 1989; Tuerk & Gold, 1990; Jellinek *et al.*, 1993; Tuerk *et al.*, 1992; Kubik *et al.*, 1994; Bock *et al.*, 1992), nucleic acids (Pei *et al.*, 1991), and small organic molecules (Ellington & Szostak, 1990, 1992; Jenison *et al.*, 1994). These techniques involve generating highly diverse libraries of oligonucleotide sequences and selecting the molecules which contain the structural features necessary for binding [reviewed in Sherman *et al.* (1993)]. The sampling of "shape space" in such libraries has proven effective for the isolation of ligands to targets which are not known to interact with nucleic acids physiologically. For example, DNA oligonucleotides that bind to the serine protease thrombin have been identified (Bock *et al.*, 1992). These DNA ligands conformed to a 14−17-base consensus sequence d(GGNTGGN$_{2-5}$GGNTGG) (N is a variable base) that has been determined by two-dimensional (2D)[1] NMR studies to fold into a unimolecular DNA quadruplex consisting of two G quartets held together by two 2-base loops and one 2−5-base loop (Macaya *et al.*, 1993; Schultze *et al.*, 1994; Wang *et al.*, 1993a,b). A recent selection for RNA ligands to thrombin identified two different structural motifs (Kubik *et al.*, 1994) that were unrelated in sequence to selected DNA ligands, confirming that the outcome of selection from DNA libraries can be different from that of RNA libraries (Ellington & Szostak, 1990, 1992).

We have repeated selection for single-stranded DNA molecules which bind to thrombin in order to determine the extent to which independent selections from DNA libraries can differ. Our selection confirmed that DNA oligonucleotides containing the previously-identified consensus quadruplex structure (Bock *et al.*, 1992) could be selected readily from such libraries. However, the DNA oligonucleotides containing this motif almost invariably contained an additional 4−7 base pairs flanking the quadruplex motif, resulting in a novel quadruplex/duplex structure. We synthesized several oligonucleotides with quadruplex/duplex motifs and tested them for thrombin binding and inhibitory activity. All quadruplex/duplex molecules tested bound to thrombin with higher affinity than molecules containing only the quadruplex motif. However, binding affinity did not always correlate with inhibition, since some quadruplex/duplex molecules were less effective in inhibiting thrombin than quadruplex structures lacking the duplex motif. ^{1}H NMR studies revealed that the complementary bases in quadruplex/duplex molecules allowed them to form multimolecular structures. In view of this observation, we followed a rational approach of bridging the 5′ and 3′ ends of the duplex motif with either triethylene glycol (TEG) or disulfide bridges to prevent the formation of multimeric structures. This approach resulted in more potent thrombin inhibitors than the previously reported oligonucleotides containing only the quadruplex motif (Bock *et al.*, 1992).

[⊗] Abstract published in *Advance ACS Abstracts,* March 15, 1995.

[1] Abbreviations: 1D, one-dimensional; 2D, two-dimensional NMR, nuclear magnetic resonance; NOE, nuclear Overhauser effect; NOESY, 2D NOE spectroscopy; P.COSY, purged correlated spectroscopy; HOHAHA, homonuclear Hartmann−Hahn spectroscopy; PAGE, polyacrylamide gel electrophoresis; HPLC, high-performance liquid chromatography; DTT, dithiothreitol; SS NOESY, NOESY acquired with symmetrically-shifted pulses replaced for the observe pulse; PCR, polymerase chain reaction; TEG, triethylene glycol; Tris, tris(hydroxymethyl)aminomethane; TEAA, triethylammonium acetate; -S−S-, disulfide bridge.

0006-2960/95/0434-4478$09.00/0

One drawback to the use of oligonucleotides as therapeutics is their susceptibility to enzymatic degradation *in vivo*. The previously-described quadruplex motif has been shown to have a half-life of approximately 2 min *in vivo* (Griffin *et al.*, 1993), and the low nuclease stability of this molecule may contribute to this short half-life. We have investigated the serum stabilities of the bridged quadruplex/duplex molecules and found them to be greatly stabilized as compared with the unbridged quadruplex. Finally, we will describe results indicating that both the length and sequence of the duplex motif of the quadruplex/duplex molecules affect inhibitory potency. Optimizing this element presents an obvious opportunity for generating even more potent thrombin-inhibiting oligonucleotides.

MATERIALS AND METHODS

General. 1-(*O*-Dimethoxytrityl)hexyl disulfide, 1′-(2-cyanoethyl)-*N*,*N*-diisopropylphosphoramidite (5′-thiol modifier-C_6 S−S), and dimethoxytrityl triethylene glycol phosphoramidite were purchased from Glen Research, Sterling, VA. Oligonucleotide HPLC purifications were performed using a Waters 600E system controller equipped with a multisolvent delivery system and a model 991 photodiode array detector. Trityl-on separations were performed using Waters RCM C_4 columns for analytical (8 mm × 10 cm) and preparative (25 mm × 10 cm) purposes. A gradient of 0.1 M triethylammonium acetate buffer (pH 7.0; TEAA, solvent A)/acetonitrile (solvent B) was used for all reversed-phase separations. Polyacrylamide gel electrophoresis (PAGE) was carried out in Tris borate buffer, pH 8, in the presence of 7 M urea. Oligonucleotide counterions were converted to the potassium salt by passage through a column of Bio-Rad AG50W-X8 resin.

Selection of Thrombin Ligands from a DNA Library. The selection of thrombin ligands from a library of single-stranded DNA sequences was carried out as described previously (Bock *et al.*, 1992) with a few minor differences in procedure. A column was prepared containing 1.2 nmol of thrombin prebound to 200 μL of concanavalin A−agarose in 20 mM Tris acetate, pH 7.4, 140 mM NaCl, 5 mM KCl, 1 mM $CaCl_2$, and 1 mM $MgCl_2$ in a 1 mL pipet; 200 μL of concanavalin A−agarose (without thrombin) was inserted into a 200 μL tip, which was placed above the pipet column, and 20 pmol of single-stranded DNA library (60-mer with randomized 30-base insert flanked by PCR primer sequences) was applied to the 200 μL precolumn in selection buffer and washed into the lower column with several column volumes of buffer. The thrombin/DNA complexes were eluted with 100 mM methyl α-D-mannoside. Fractions containing thrombin were identified by assay with the chromogenic substrate S-2238 (Pharmacia, 160 Industrial Dr., Franklin, OH 45005). The fractions containing thrombin were combined and extracted with phenol, and the complexed oligonucleotides were precipitated from ethanol. Oligonucleotides were amplified asymmetrically using 200 pmol of primer d(CCGAAGATGTCTACT) and 5 pmol of primer d(CCGAAGAACAGATGT). Single-stranded oligonucleotides were purified by agarose gel electrophoresis prior to each round of selection. Complexed oligonucleotides were amplified after six rounds of selection using the cloning primers d(CCGAATTCTCGAGCCGAAGAACAGATGT) and d(CCGAATTCTAGACCGAAGATGTCTACT); the products were digested with *Eco*R1 and *Xba*1 and cloned into the *Eco*R1/*Xba*1 sites in pUC19. Plasmids were sequenced by chain termination sequencing using Sequenase (U.S. Biochemicals).

Oligonucleotide Synthesis. Oligonucleotides were prepared on an Applied Biosystems model 394 DNA synthesizer on a 1 μmol scale. Unmodified oligonucleotides were purified by trityl-on HPLC followed by detritylation, extraction, ethanol precipitation, and conversion to the potassium salt using AG50W-X8 resin. Triethylene-glycol-bridged oligonucleotides were prepared as previously described (Gao *et al.*, 1994). These oligonucleotides were purified by reversed-phase HPLC. Disulfide-bridged oligonucleotides were prepared as previously described (Gao *et al.*, 1995). The desired material was isolated by preparative PAGE electrophoresis (21 cm × 12 cm × 1.5 mm), extracted from the gel with 0.3 M sodium acetate (pH 5.2), filtered, and precipitated from 80% ethanol. Each purified product migrated as a single band on a denaturing PAGE gel. The oligonucleotides synthesized are listed in Table 1. In addition, three oligonucleotides in which deoxyinosine was substituted for deoxyguanosine were synthesized for NMR purposes, one of which also contained a deoxyuridine for deoxythymidine substitution. These oligonucleotides were also bridged with TEG at the end of the duplex structure but were not ligated, so that they contained a "nick" (unligated 5′ and 3′ ends) between the fourth and fifth base pairs of the duplex motif. The sequences of these molecules, using the numbering scheme from Figure 7A to indicate the positions of the deoxyinosine and deoxyuridine substitutions, are I11, d(GTGACTACTGITTGGTGAGGTTGGGTAGT-CAC-TEG); I24, d(GTGACTACTGGTTGGTGAGGTT-GIGTAGTCAC-TEG); and I3-U29, d(GTIACTACTGGT-TGGTGAGGTTGGGTAGUCAC-TEG).

Thrombin-Binding Studies. DNA oligonucleotides to be tested were labeled using T4 polynucleotide kinase and excess [γ-^{32}P]ATP and purified on an 8% denaturing PAGE gel. Labeled DNA oligonucleotides were gel purified and quantified on the basis of the incorporated label. The percent binding of oligonucleotides to thrombin was determined at 680, 68, and 6.8 nM protein concentrations in 20 μL of selection buffer (140 mM NaCl, 5 mM KCl, 1 mM $MgCl_2$, 1 mM $CaCl_2$, 20 mM Tris acetate, pH 7.4) containing approximately 40−50 fmol (2−2.5 nM) of DNA for each oligonucleotide tested (usually about 30 000 cpm). The fraction of "active" thrombin in the mixture was determined from the titration of thrombin protein in the binding mixtures with a fixed oligonucleotide concentration to be approximately 18%. The binding curve plots were then corrected to the concentration of "active" thrombin. Mixtures were incubated for 30 min at room temperature and then filtered through nitrocellulose filters. Labeled DNA retained on filters was counted, and the percent DNA bound was determined after subtracting background binding to filters (cpm retained on filters in the absence of protein).

Competition Studies. The 15-mer oligonucleotide d(GGTTGGTGTGGTTGG) (oligonucleotide **2**) was labeled and purified as described above. Competition binding studies were carried out by determining the percent labeled (about 84 fmol) 15-mer DNA bound at 680 nM *total* thrombin protein concentration as described above, in the presence of approximately 0-, 60-, 120-, 240-, 480-, or 1200-fold excess of unlabeled competitor DNA.

Table 1: Structures and Sequences of Bridged and Unbridged Oligonucleotides

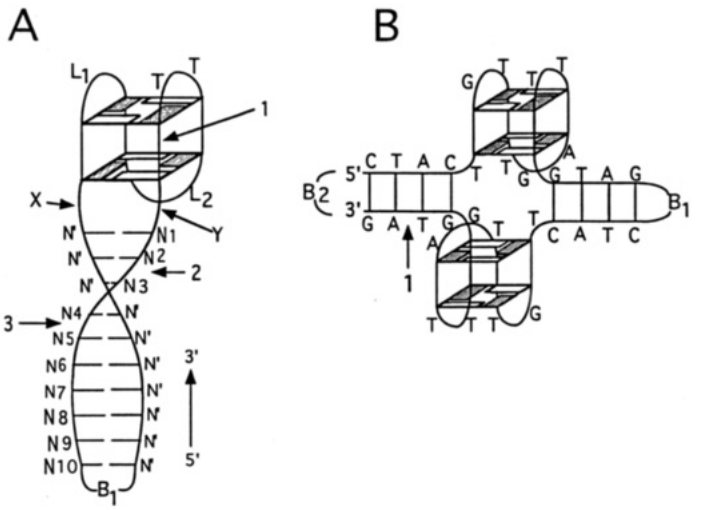

oligonucleotide	length	structure[a]	L1[b]	L2[b]	X[c]	Y[c]	B1[d]	B2[d]	nick[e]	no. of bp[f]	stem sequence[g]
1	15-mer	A	TT	TGA						0	
2	15-mer	A	TT	TGT						0	
3	24-mer	A	GT	TGA	T					4	GTAG
4	24-mer	A	GT	TGA	T		TEG		2	4	GTAG
5	24-mer	A	GT	TGA	T		TEG		1	4	GTAG
6	24-mer	A	GT	TGA	T		TEG			4	GTAG
7	32-mer	A	TT	TGA	T		TEG		3	8	GTAGTCAC
8	32-mer	A	TT	TGA	T					8	GTAGTCAC
9	32-mer	A	TT	TGA	T		TEG			8	GTAGTCAC
10	36-mer	A	TT	TGT	T					10	GTAGCATCGC
11	48-mer	B					TEG			4	
12	48-mer	B					TEG	TEG	1	4	
13	15-mer	A	TT	TGA			-S−S			0	
14	20-mer	A	TT	TGA	T		-S−S-			2	GT
15	24-mer	A	TT	TGA	T		-S−S-			4	GTAG
16	24-mer	A	GT	TGA	T		-S−S-			4	GTAG
17	26-mer	A	TT	TGA	T		-S−S-			5	GTAGT
18	28-mer	A	TT	TGA	T		-S−S-			6	GTAGTC
19	30-mer	A	TT	TGA	T		-S−S-			7	GTAGTCA
20	30-mer	A	TT	TGA	T		-S−S-			7	GTAACAT
21	38-mer	A	TA	GATA	CT	TGC	-S−S-			7	TAGACAT
22	32-mer	A	TT	TGA	T		-S−S-			8	GTAGTCAC
23	34-mer	A	TT	TGA	T		-S−S-			9	GTAGTCACT
24	36-mer	A	TT	TGA	T		-S−S-			10	GTAGTCACTG

[a] Class of structure for each molecule (illustrated above the table). [b] Nucleotide sequences in the corresponding loops in structure A. [c] Non-base-paired sequences at the quadruplex/duplex junction in structure A. [d] Class of bridging moiety [triethylene glycol (TEG) or disulfide (-S−S-)]. [e] Position in structure A or B of any unligated 5′−3′ ends. [f] Number of base pairs in the duplex−stem motif. [g] Sequence of the duplex−stem starting at the N1 position in structure A.

Thrombin Inhibition Assays. (1) Clotting Assay. The assay for the inhibition of thrombin-catalyzed fibrin clot formation was performed as previously described (Bock *et al.*, 1992). Thrombin with an activity of 4080 units/mg of protein and fibrinogen (fraction 1, type 1 from human plasma) were purchased from Sigma. Human fibrinogen in selection buffer (140 mM NaCl, 5 mM KCl, 1 mM $MgCl_2$, 1 mM $CaCl_2$, 20 mM Tris acetate, pH 7.4, 200 μL) was equilibrated at 37 °C for 1 min in the presence of each oligonucleotide. Reactions were initiated by the addition of human thrombin (100 μL in selection buffer pre-equilibrated to 37 °C for 1 min) to final concentrations of 2 mg/mL fibrinogen and 13 nM thrombin. The first indication of a clot was taken as clotting time. Clot formation was usually complete within 5 s of the first appearance of a clot.

(2) Activity Assay for DNA Stability in Serum. Inhibition assays using DNA oligonucleotides which were preincubated in human serum were carried out by adding fibrinogen mixture (200 μL in selection buffer) to 100 μL of oligonucleotide-containing serum after a 1 h incubation at 37 °C and then adding thrombin (100 μL in selection buffer) to initiate the clotting reaction. These studies were carried out in order to determine the extent to which inhibitory activity was retained after exposure to serum. Final concentrations for fibrinogen and thrombin were 1.5 mg/mL and 9.75 nM, respectively, in 400 μL.

(3) Fibrinopeptide A Release Assay. The inhibition of the thrombin-catalyzed release of fibrinopeptide A was carried out in a manner similar to that previously described (Ng *et al.*, 1993). Clotting reaction mixtures (300 μL) were initiated exactly as described above, but the reactions were quenched 40 s after initiation of the reaction and prior to clot formation by the addition of 100 μL of 3 M perchloric acid. Water (100 μL) was added, and the mixtures were centrifuged at 10000*g* for 5 min at room temperature. An aliquot (450 μL)

of the supernatant was analyzed by reversed-phase HPLC (4.6 × 250 mm, Whatman, PartiSphere C_{18}). Fibrinopeptides were eluted from the column at room temperature using a gradient of solvent B in 0.08 M sodium phosphate (pH 3.1) at a flow rate of 1 mL/min. The elution gradient employed 17% acetonitrile (solvent B) over 15 min, 17−40% over 10 min and held at 40% for 5 min, and then 40−70% over 1 min and held at 70% for 3 min. The retention times for fibrinopeptides A and B were determined using standards (Sigma). Fibrinopeptide A eluted as a well-resolved peak and was quantitated by integration of its absorption peak at 205 nm using Millenium 2010 Chromatography Manager V2.00 system software.

NMR Spectroscopy. ^{1}H NMR spectra were acquired at 500 MHz on a Varian UNITY-*plus* spectrometer. One-dimensional (1D) spectra of samples dissolved in 90% H_2O/10% D_2O were acquired using symmetrically-shifted (SS) shaped pulses to suppress the water resonance (Smallcombe, 1993). Samples in D_2O were prepared by drying the sample using a stream of nitrogen gas and redissolving in 99.996% D_2O. NOESY spectra in D_2O were acquired in the phase-sensitive mode (States *et al.*, 1982) using the standard pulse sequence (Kumar *et al.*, 1980) with presaturation of the water resonance during the recycle delay. P.COSY spectra were acquired using a full 90° flip angle pulse (Marion & Bax, 1988). HOHAHA spectra were acquired as described by Davis and Bax (1985) using the required number of MLEV17 cycles (Levitt *et al.*, 1982; Bax & Davis, 1985) to achieve the desired spin−lock time. SS NOESY spectra in water were acquired in the phase-sensitive mode using symmetrically-shifted shaped pulses (Smallcombe, 1993). Spectra were processed using Varian VNMR processing software (version 4.2A). Linear prediction was used to eliminate large frequency-dependent phase shifts from spectra acquired using SS pulses. Solvent subtraction was used to subtract the residual water resonance from the FID. Spectra were referenced with respect to the chemical shift of water calibrated to DSS for the sample conditions used. Specific acquisition or processing parameters are presented in the figure legends.

Stability of Bridged Oligonucleotides in Serum. Aliquots of each oligonucleotide (0.9 OD_{260}) were mixed with pure human serum (final oligonucleotide concentration in serum = 0.5 μM). After incubation at 37 °C for specific time periods, the samples were analyzed by ion-exchange HPLC (Dionex NucleoPac PA-100, 4 × 250 mm) with a linear gradient from 0 to 1.0 M ammonium chloride in 25 mM Tris-HCl, pH 8.0, 0.5% acetonitrile at a flow rate of 1.5 mL/min. Peak area of the intact oligonucleotide as a percentage of starting area was plotted versus time to calculate the half-life ($t_{1/2}$) of the oligonucleotide.

UV Melting Studies. Oligonucleotide (0.5 OD) was dissolved in 0.5 mL of 10 mM potassium phosphate buffer (pH 7.0). Samples were heated to 100 °C for 5 min and then allowed to cool to room temperature. UV melting profiles were measured at 260 nm on a Gilford Response II temperature-controlled spectrophotometer from 20 to 100 °C at a rate of 0.8 °C/min. The melting transition temperatures were obtained from a first-derivative plot of absorbance versus temperature.

RESULTS AND DISCUSSION

Selection of a Novel Quadruplex/Duplex DNA Structure. The selection procedure for single-stranded DNA ligands to thrombin was carried out as described above. Initial sequencing identified 18 unique sequences (Figure 1A) which contained the previously-reported 14−17-base consensus sequence d(GGNTGGN$_{2-5}$GGNTGG), where N is a variable base position, for DNA ligands to thrombin (Bock *et al.*, 1992). DNA oligonucleotides conforming to this consensus sequence have been shown by NMR studies to fold into unimolecular DNA quadruplexes containing two G quartets held together by three loops (Macaya *et al.*, 1993; Schultze *et al.*, 1994; Wang *et al.*, 1993a,b) (Figure 1B). However, the oligonucleotides that were isolated in this selection also contained four to seven complementary bases flanking the quadruplex motif, indicating the potential to form a novel DNA structure consisting of a quadruplex with an adjacent duplex motif (Figure 1A,C). Usually one to three unpaired nucleotides were located at the putative quadruplex−duplex junction, although in at least one case there were no unpaired nucleotides at this junction. The quadruplex portion of this novel consensus structure contained two to three nucleotides, at least one of which was T, in each of the two loops on the same side of the quadruplex, whereas the previous quadruplex consensus sequence always contained two nucleotides in these loops, with the 3′ base in each always being a T. The finding that each of the two loops in the new consensus motif always contained a T nucleotide is consistent with the presence of an unusual T−T base pair between the two loops (Macaya *et al.*, 1993; Schultze *et al.*, 1994; Padmanabhan *et al.*, 1993), even when one of the loops contained three bases. Although there was no obvious consensus sequence in the duplex−stem, the sequences 5′-ATGT-3′ and 5′-GTAG-3′ were both found in the duplex motif of 3 of the 18 unique sequences (without allowing for mismatches or bulges), suggesting that duplex−stems containing these sequences may have exhibited a higher binding affinity for thrombin during the selection procedure. However, the importance of these sequences is difficult to assess since in each case the sequence forms base pairs with one of the nonrandomized flanking sequences used for PCR purposes and therefore may be superior sequences only in the context of these flanking sequences. It is possible that there is an optimal consensus sequence for the duplex motif, but the selection did not identify such sequences. The starting frequency of such optimal sequences in the original oligonucleotide population would be significantly lower than in oligonucleotides with a nonoptimal duplex and therefore could require more rounds of selection for their identification. Additional rounds of selection may have led to the identification of such an optimal duplex sequence. Another possibility is that the stringency of the selection may have been insufficient to provide a competitive advantage to optimal duplex sequences compared to the identified oligonucleotides. Finally, it is always possible that procedural or artifactual losses of certain sequences could skew the final outcome of *in vitro* selections.

Duplex Motif Confers Higher Binding Affinity. DNA molecules conforming to the consensus quadruplex/duplex structure illustrated in Table 1 were synthesized and tested for their affinity to thrombin using thrombin-dependent binding curves. Oligonucleotides containing the novel

A

CCGAAGATGTCTACTACAGTGTTACT**GGTTGGATCGGTATGG**CAAACATCTGTTCTTCGG
CCGAAGATGTCTACTGATCTGCTT**GGTTGGGAAGGTTTGG**GAAGCACATCTGTTCTTCGG
CCGAAGATGTCTACTATGTGAGTGTT**GGTTGGGAAGGTTGG**TCGAACATCTGTTCTTCGG
CCGAAGATGTCTACTTA**GGTTGGTGTGGATGG**AAGTGGACATTTAACATCTGTTCTTCGG
CCGAAGATGTCTACTAGCATGTGTT**GGTTGGGCAGGTATGG**GTACACATCTGTTCTTCGG
CCGAAGATGTCTACTATG**GGGTGGTTCGGTTGG**CATAGTGATCGTACATCTGTTCTTCGG
CCGAAGATGTCTACTTATGGTTA**GGTTGGTTCTCGGTTCG**TAGACACATCTGTTCTTCGG
CCGAAGATGTCTACTGATGGTTAATTT**GGCTGGGTAGGTTGG**TTAACATCTGTTCTTCGG
CCGAAGATGTCTACTACTT**GGTAGCGTTGGTTTGA**TCTTGTTTATACATCTGTTCTTCGG
CCGAAGATGTCTACTGCAGAGTGTAA**GGTTGGGTATGGTTTGG**GTACATCTGTTCTTCGG
CCGAAGATGTCTACTGTACATATGTAAT**GGATTGGGAGGGTGG**TTACATCTGTTCTTCGG
CCGAAGATGTCTACTTGCAATTA**GGTTGGTTAGGCTTGG**TTTGCAACATCTGTTCTTCGG
CCGAAGATGTCTACTCAGAGTTAGCA**GGGTGGATTGGTTGG**TGCTACATCTGTTCTTCGG
CCGAAGATGTCTACTA**GGTTGGCTTGGGTTGG**GGGTAGCGATGGCACATCTGTTCTTCGG
CCGAAGATGTCTACTA**GGTTGGCTAGGGTTGG**TGTAGGAGATGGCACATCTGTTCTTCGG
CCGAAGATGTCTACTGATTGACT**GGTTGGTGCAGCTTGG**TTTGTCACATCTGTTCTTCGG
CCGAAGATGTCTACT**GGGTGGTGAGGTTGG**GTAGCACTGATGTAAACATCTGTTCTTCGG
CCGAAGATGTCTACT**GGTAGGGATAGGTTGG**TGCTAGACATGATACATCTGTTCTTCGG

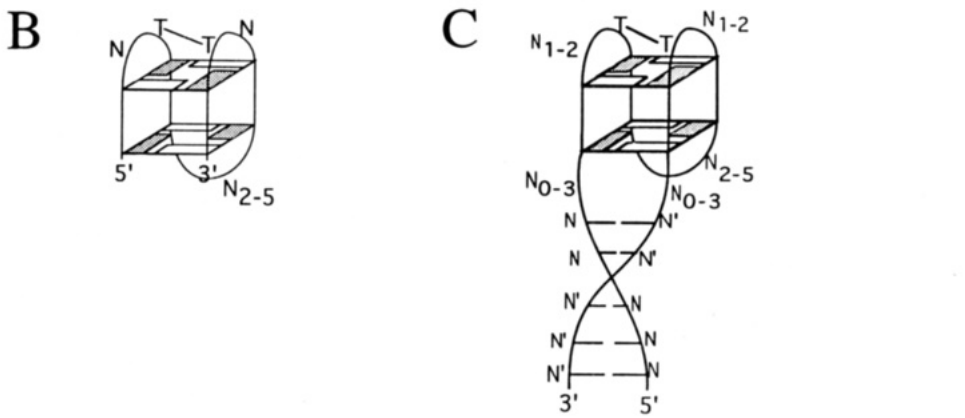

FIGURE 1: (A) Sequences identified by selection from DNA ligands to thrombin. Bold letters identify the sequences which conform to the previously-identified consensus sequence (Bock *et al.*, 1992), and underlined bases identify the complementary sequences flanking the quadruplex consensus. The boundaries of the randomized region from the library of DNA sequences used in the selection are indicated by arrowheads. (B) Consensus structure of the previously-identified DNA ligands (Bock *et al.*, 1992). Rectangles indicate the G residues involved in quadruplex formation. Shaded rectangles indicate *syn* G nucleotides. N indicates a variable base position. The dash between the two Ts indicates a T·T base pair. (C) One potential conformation of the newly-identified consensus motif. N indicates a variable base composition and N′ indicates its Watson−Crick base-pairing partner. The duplex−stem length varied between 4 and 7 base pairs.

quadruplex/duplex motif (oligonucleotides **3**, **4**, **7**, and **8**) were estimated to have K_D values of approximately 10−25 nM, which is a 4−10 times higher affinity than our estimate of 100 nM for the K_D of the isolated quadruplex motif (oligonucleotide **2**) from these binding curves (Figure 2A). A quadruplex/duplex molecule with a "nick" (unligated 5′ and 3′ ends) between adjacent G nucleotides within the quadruplex motif (oligonucleotide **5**) bound poorly ($K_D \approx 1$ μM), probably due to the inability of such a "nicked" quadruplex to form a stable structure (Figure 2A). This result indicates that although the duplex−stem motif can enhance binding in quadruplex/duplex molecules, it alone is not sufficient for thrombin binding at the concentrations tested.

Quadruplex/Duplex Oligonucleotides Bind to the Anion Binding Exosite on Thrombin. Previous work has indicated that the thrombin binding site for the 15-mer quadruplex d(GGTTGGTGTGGTTGG) is the anion binding exosite, also called the fibrinogen recognition exosite (Wu *et al.*, 1992; Paborsky *et al.*, 1993; Padmanabhan *et al.*, 1993). A competition study (Figure 2B) determined that the higher affinity exhibited by quadruplex/duplex molecules was not due to binding to a different site on thrombin, since a molecule containing the duplex−stem motif (oligonucleotide **9**) competed for binding with that possessing only the quadruplex motif. Such a result is not surprising since the quadruplex motif, which is sufficient for binding to this site, is present in all competing molecules, and it is highly unlikely that a structure containing this motif would be selected to bind to a different site. The finding that a control oligonucleotide with a random 15-base sequence did not compete with binding of the quadruplex 15-mer indicates that the competition observed for the other tested oligonucleotides is not due to nonspecific binding. The higher affinity of the quadruplex/duplex structure is therefore probably due to additional or improved protein contacts made by this oligonucleotide structure at the anion binding exosite on thrombin.

Thrombin Inhibition. Several DNA oligonucleotides were tested for their ability to inhibit thrombin activity as measured by an extension of the time for thrombin-catalyzed fibrin clot formation (Table 2). These tests revealed that thrombin-binding affinity did not always correlate with inhibition. For example, the quadruplex/duplex with a 4-base-pair stem (oligonucleotide **3**) bound thrombin with an approximately 10-fold higher affinity than the isolated quadruplex motif (oligonucleotide **2**) (Figure 2A) but was not more effective at inhibiting thrombin than the isolated quadruplex (Table 2). This paradox suggested that either the optimal protein

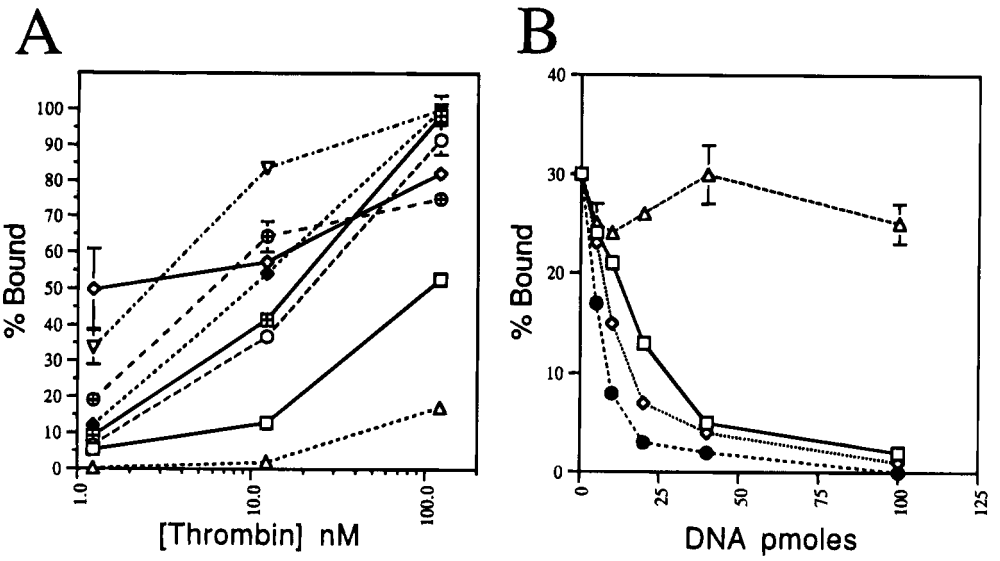

FIGURE 2: (A) Oligonucleotide binding as a function of thrombin concentration. Sequences and structures can be identified from Table 1. Symbols for oligonucleotides are as follows: (□) 15-mer quadruplex (oligonucleotide **2**); (◇) 24-mer quadruplex/duplex (oligonucleotide **3**); (○) 24-mer with TEG bridge, nicked stem (oligonucleotide **4**); (△) 24-mer with TEG bridge, nicked quadruplex (oligonucleotide **5**); (□ with +) 32-mer with TEG bridge, nicked 8-base-pair stem (oligonucleotide **7**); (◆) 32-mer with 8-base-pair stem (oligonucleotide **8**); (⊕) 48-mer unimolecular "dimer mimetic", with two TEG bridges, one nicked 4-base-pair stem (oligonucleotide **12**); and (▽) 48-mer "dimer mimetic" with one TEG bridge (oligonucleotide **11**). All points are normalized with respect to the binding plateau for each oligonucleotide. (B) Binding competition between ^{32}P-labeled 15-mer (oligonucleotide **2**) and several sequences: (□) unlabeled 15-mer (oligonucleotide **2**) (itself); (◇) quadruplex/duplex with TEG-bridged, ligated 8-base-pair stem (oligonucleotide **9**); (●) unimolecular "dimer mimetic" (oligonucleotide **11**); and (△) scrambled 15-mer d(GGTGGTGGTTGTGGT). Percent bound was calculated for labeled ("hot") 15-mer as described in Materials and Methods. Points represent the average of duplicate measurements for both binding and competition studies, and error bars are indicated.

Table 2: Thrombin-Inhibitory Activity and T_m of Oligonucleotides

oligonucleotide	no. of bp	[DNA] (nM)	[thrombin] (nM)	clotting time[a]	% fib. A release[b]	T_m (°C)[c]
none				37		
1	0	100	13	123		NT[d]
2	0	100	13	172		NT
3	4	100	13	124		NT
15	4	100	13	368		60
8	8	100	13	397		42
9	8	100	13	445		63
22	8	100	13	428		73
10	10	100	13	189		52
24	10	100	13	488		73
19	7	100	13	357		71
20	7	100	13	385		64
21	7	100	13	49		60
none			6		100	
9	8	100	6		8.2	
9	8	20	6		26	
9	8	10	6		46.3	
1	0	100	6		29.7	

[a] Clotting time in seconds determined as described in Materials and Methods. [b] Percent fibrinopeptide A released compared to control clotting reaction (no oligonucleotide). [c] Temperature at which UV melting transition is 50% complete. [d] No UV melting transition observed.

contacts for binding and inhibition are different or, alternatively, that differences between the binding and inhibition assay conditions result in differences in the observed interaction between the target (thrombin) and the ligand (oligonucleotide).

NMR Studies Reveal Formation of Multiple Quadruplex/Duplex Structures. NMR studies of the 24-mer d(CTACTGGGTGGTGAGGTTGGGTAG) (oligonucleotide **3**) demonstrated that this sequence formed two predominant structures in solution. This was indicated by the appearance of more hydrogen-bonded imino proton resonances than would be expected for a single duplex/quadruplex structure (Figure 3A). For example, the duplex−stem of the predicted quadruplex/duplex structure contains only two Watson−Crick base-paired guanines, and therefore only two imino proton resonances corresponding to these two nucleotides should be present in the NMR spectrum. The appearance of more than two such G imino resonances in the imino proton region of the spectrum (Figure 3A) indicated the presence of other structures in solution. The presence of twice the number of $C(H_5)-C(H_6)$ cross-peaks in a P.COSY (Marion & Bax, 1988) spectrum (data not shown) confirmed that two predominant structures were present. Both structures appeared to contain quadruplex motifs since more than eight resolved intrabase G amino proton pairs were evident in a NOESY (Kumar *et al.*, 1980; Smallcombe, 1993) spectrum in H_2O (data not shown). The presence of resolved NOEs between G amino protons and slowly exchanging G imino protons is characteristic of G quadruplexes (Smith & Feigon, 1992), and only a maximum of eight such G amino proton pairs would be expected if a single unimolecular structure predominated. In addition, there were more than the eight Hoogsteen base-paired G imino resonances expected for a single unimolecular quadruplex structure, indicating the presence of more than one quadruplex species (Figure 3A). These findings are consistent with the presence of two structures, a unimolecular duplex/quadruplex and a bimolecular duplex/quadruplex structure, held together by intermolecular base pairing (Figure 3C). Further evidence for the formation of such multimeric structures was obtained by varying the sample conditions. The combination of dilution of the oligonucleotide, quick heating and reannealing, lowering salt concentration, and the addition of Mg^{2+} ion appeared to shift the equilibrium toward the monomeric form, as evidenced by the appearance in the proton spectrum of

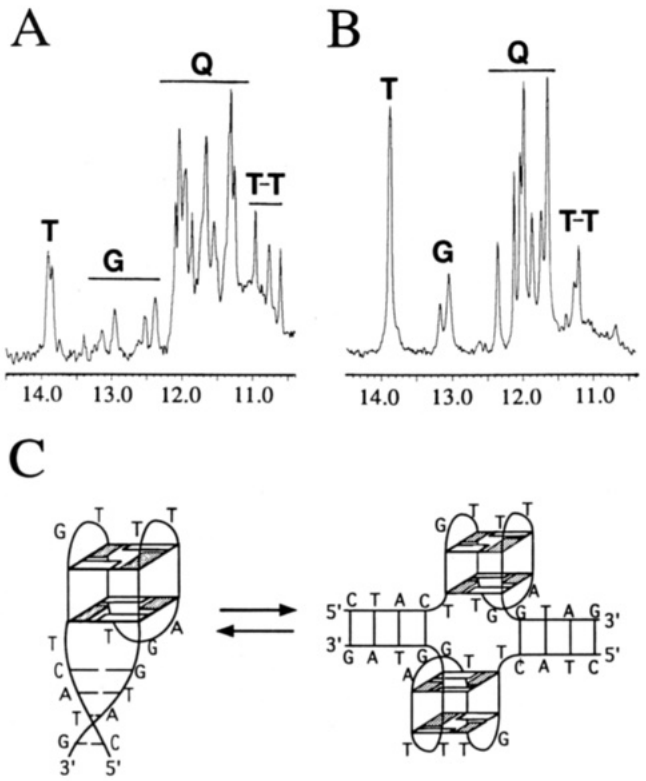

FIGURE 3: (A, B) One-dimensional ^{1}H NMR spectra of the H-bonded imino proton resonances of the 24-mer quadruplex/duplex d(CTACTGGTTGGTGAGGTTGGGTAG) (oligonucleotide **3**) with a 4-base-pair duplex motif at 1 °C. H-bonded imino proton resonances were classified as Watson−Crick T iminos (T), Watson−Crick G iminos (G), Hoogsteen base-paired quadruplex G iminos (Q), or T−T base-paired T iminos (T−T). Sample conditions were 1.9 mM DNA, 88 mM KCl (A) and 0.12 mM DNA, 6.9 mM $MgCl_2$, 6.1 mM KCl (B) at pH 6.1 in 90% H_2O/10% D_2O. The sample for panel B was heated to 90 °C and quickly cooled to 1 °C. Spectra were acquired at 500 MHz as the first increment of an SS NOESY (Smallcombe, 1993). Sweep widths were 11 000 Hz. Spectra were acquired with 4096 complex points and 64 (A) or 16 384 (B) acquisitions using a 208 μs SS pulse (Smallcombe, 1993), processed by linear prediction of the first two data points of the FID, zero-filling to 8192 points and solvent subtracting the residual water peak, and apodized using a shifted Gaussian window function. Axis units are ppm. (C) Scheme of the two predominant structures proposed for oligonucleotide **3** at equilibrium. Rectangles represent guanine bases forming a G quartet. Shaded rectangles indicate *syn* G nucleotides.

the expected number of H-bonded imino proton resonances for this structure (Figure 3B). The discrete sets of resonances for these two proposed structures indicate that the rate of interconversion between the structures at equilibrium is longer than the NMR time scale. Such dynamics are typical of oligonucleotides containing self-complementary sequences capable of forming both hairpin and bimolecular duplex structures (Orbons *et al.*, 1987; Blommers *et al.*, 1989; Boulard *et al.*, 1991; Kallick & Wemmer, 1991; Gupta *et al.*, 1993; Glick, 1991). In this context, the unimolecular quadruplex/duplex structure could be considered to be a hairpin with a highly-structured loop, thus making the quadruplex motif the most structured loop reported to date. The formation of the multimeric structure described above may be limited to molecules which are not conformationally trapped as a stable unimolecular structure.

Synthesis of Bridged Oligonucleotides. In order to constrain quadruplex/duplex molecules to the unimolecular structure, a series of oligonucleotides was synthesized in which the 5′ and 3′ ends of the duplex−stem were covalently linked by either a triethylene glycol (TEG) bridge (oligonucleotides **4**−**7**, **9**, **11**, and **12**) or a disulfide-containing poly(methylene) bridge (-S−S-) (oligonucleotides **14**−**24**) (Table 1). Similar strategies have been used to constrain a unimolecular DNA hairpin (Glick 1991, 1992; Gao *et al.*, 1995). The synthesis of circular (no 5′−3′ "nick") TEG-bridged sequences was accomplished by chemical ligation of the ends of the oligonucleotide using a water-soluble diimide as the coupling agent. This procedure required that portions of the sequence were held in a double-stranded conformation by base pairing to facilitate formation of the phosphodiester bond. This method was suitable for oligonucleotides possessing 8 base pairs such as oligonucleotide **9**, since the duplex was stable under the conditions of the ligation, but was less successful for sequences with shorter stem regions such as oligonucleotide **6**, with a 4-base-pair stem, for which the yield of the ligated product was significantly lower. Previous studies (Gao *et al.*, 1994) have shown that ligation of TEG-bridged duplexes can be accomplished efficiently with 12-base-pair duplexes. It is interesting to note that oligonucleotide **5**, possessing a nick in the quadruplex region, could not be ligated by this procedure, presumably because the structure was too unstable with a nick between adjacent guanine nucleotides. In all cases, the ligated product migrated more rapidly than its unligated counterpart on denaturing PAGE and could be purified by elution from the gel.

Disulfide-bridged oligonucleotides were prepared by synthesizing molecules with sulfhydryl groups attached to the ends via aliphatic, six-carbon linkers and oxidizing the sulfhydryls in air overnight. This procedure was effective in producing a wide variety of bridged oligonucleotides (oligonucleotides **14**−**24**) even when the base-paired region was very short. In fact, a bridged quadruplex alone (oligonucleotide **13**) was also prepared by this procedure.

Bridging the Duplex−Stem Results in More Potent Inhibitors. The series of constrained unimolecular quadruplex/duplex molecules proved to be significantly better thrombin inhibitors than the 15-mer oligonucleotides exhibiting only the quadruplex motif (oligonucleotides **1** and **2**). In a direct comparison of thrombin inhibition using a clot formation assay, the molecule containing the 8-base-pair stem bridged by TEG (oligonucleotide **9**) was as inhibitory as a 5-fold higher concentration of the 15-mer quadruplex (oligonucleotide **2**) reported previously (Bock *et al.*, 1992) (Figure 4). When the clot formation assay employed 6 nM thrombin, 50% inhibition (*i.e.*, IC_{50}) for oligonucleotide **9** was found to be 6 nM. The same comparative 5-fold difference in the inhibitory potency of the quadruplex/duplex structure (oligonucleotide **9**) versus the quadruplex alone (oligonucleotide **2**) was obtained when release of fibrinopeptide A was used to measure thrombin activity (Table 2). The finding that the quadruplex/duplex molecules with an unbridged (oligonucleotide **8**) or a bridged but "nicked" (oligonucleotide **7**) 8-base-pair stem are more effective inhibitors than the 15-mer quadruplex (oligonucleotide **2**) (Table 2) suggests that these oligonucleotides, containing an 8-base-pair duplex, do not form multimeric structures to an appreciable extent. NMR studies on oligonucleotides **7** and **8** confirmed this (data not shown). The binding data is more closely correlated with inhibitory potency for these two molecules. However, bridging the duplex ends of oligonucleotide **8** to form

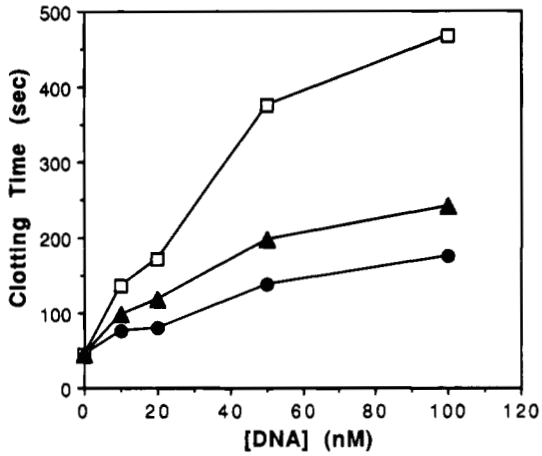

FIGURE 4: Clotting time versus DNA concentration (nM) for (□) the 32-mer TEG-bridged, ligated quadruplex/duplex molecule (oligonucleotide **9**) (illustrated in Figure 7A), (●) the isolated 15-mer quadruplex motif d(GGTTGGTGAGGTTGG) (oligonucleotide **1**), and (▲) the 48-mer unimolecular "dimer mimetic" (oligonucleotide **11**) (illustrated as structure B in Table 1). Clotting times represent single time points measured as described in Materials and Methods.

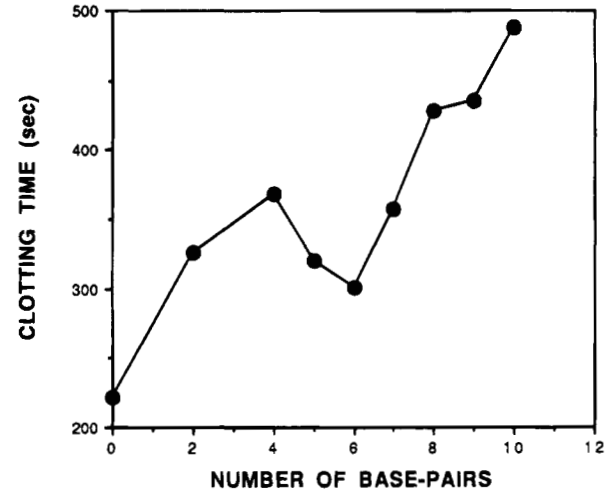

FIGURE 5: Plot of clotting time as a function of number of base pairs in the duplex−stem motif for disulfide-bridged quadruplex/duplex molecules of a specific sequence. The molecules tested in this study are oligonucleotides **13**−**15**, **17**−**19**, and **22**−**24** for stem−duplex motifs containing 0, 2, and 4−10 base pairs, respectively. Clotting times were determined at 13 nM thrombin and 100 nM oligonucleotide as described in the text. Clotting time points consist of single measurements which are representative of the relative potency of the tested oligonucleotides from several such studies.

oligonucleotides **9** (TEG-bridged) or **22** (disulfide-bridged) still did increase its inhibitory activity, though not as significantly as for shorter duplex motifs (Table 2).

Quadruplex/Duplex "Dimer Mimetics". Oligonucleotides **11** and **12**, whose folded conformations are predicted to mimic dimeric structures (illustrated in structure B in Table 1), were prepared in order to determine the binding and the inhibitory activities of these types of structures. These dimer mimetics consisted of two 24-mer oligonucleotides (of the same sequence as oligonucleotide **3**) in tandem, with a triethylene glycol linker spanning one or both duplex−stems (oligonucleotides **11** and **12**, respectively). Both of these "dimer mimetics" bound to thrombin with K_D values possibly as good as 5 nM, a 2−5-fold higher affinity than that for the quadruplex/duplex oligonucleotides tested (Figure 2A), but were only comparable to the isolated quadruplex oligonucleotide (oligonucleotide **2**) at inhibiting thrombin (Figure 4). The "dimer mimetic" molecules also compete for the same binding site on thrombin (Figure 2B). The finding that the unimolecular "dimer mimetics" bound thrombin with the highest affinities (Figure 2) but were not comparably potent inhibitors (Figure 4) indicates that quadruplex/duplex dimers contain all the structural features for thrombin binding but probably lack additional thrombin contacts needed for improved thrombin inhibition. The finding that the "dimeric mimetic" (oligonucleotide **11**) was a slightly better inhibitor than oligonucleotide **1** (Figure 4) is calculated on a *per molecule* basis. Considering oligonucleotide **11** as two separate "strands" connected by TEG would double the "strand" concentration indicated in Figure 4 and make the inhibitory potency of oligonucleotide **1** comparable to that of oligonucleotide **11**. These results are consistent with the quadruplex/duplex molecule (oligonucleotide **3**) not possessing a higher potency than the quadruplex oligonucleotides **1** and **2** (Table 2), despite its higher affinity for thrombin (Figure 2A) due, in part, to the formation of quadruplex/duplex dimeric structures. However, it is also possible that some other unknown phenomenon is the cause for the discrepancy between the binding and inhibition data for oligonucleotide **3**.

Importance of Duplex−Stem Length and Sequence. As a preliminary approach to evaluate the importance of the duplex stem sequence, a series of disulfide-bridged quadruplex/duplex molecules with varying lengths of base-paired stems were synthesized. Thus, oligonucleotides **13**−**15**, **17**−**19**, and **22**−**24** were prepared with 0-, 2-, and 4−10-base-pair duplex motifs, respectively (Table 1). In addition, three oligonucleotides (**19**−**21**) were prepared with 7-base-pair duplexes of different sequence. Thrombin inhibition was found to increase with the length of the duplex stem from 0 to 4 base pairs and also from 7 to 10 base pairs. Little difference was found for duplex motifs of length 4−7 base pairs (Figure 5). This profile of inhibitory activity as a function of the number of base pairs suggests that the enhanced inhibition observed by the addition of up to 4 base pairs may be due to stabilization of the quadruplex motif. Under the conditions of selection, additional base pairs up to 7 may confer little selective advantage. The further increase in inhibition found when the duplex is extended from 7 to 10 base pairs therefore is not likely to be the result of stabilization, implying that this enhancement may be due to additional protein contacts or more effective exclusion of fibrinogen from the fibrinogen recognition site by the extended motif. Surprisingly, quadruplex/duplex oligonucleotides with 4- and 8-base-pair duplex−stem motifs bind with approximately equal affinity to thrombin. Therefore, duplex motifs with 8 base pairs would not have a selective advantage, thus providing one explanation for the lack of such longer duplex motifs among the identified sequences.

The disulfide-bridged quadruplex (oligonucleotide **13**) was a better inhibitor than the unbridged quadruplex (oligonucleotide **1**) (Table 2), indicating that constraining the quadruplex motif improves inhibition. However, the finding that all quadruplex/duplex structures which were constrained by a disulfide bridge (oligonucleotides **14**, **15**, **17**−**19**, and **22**−**24**) were more potent inhibitors than the disulfide-bridged quadruplex motif alone (oligonucleotide **13**) (Figure 5)

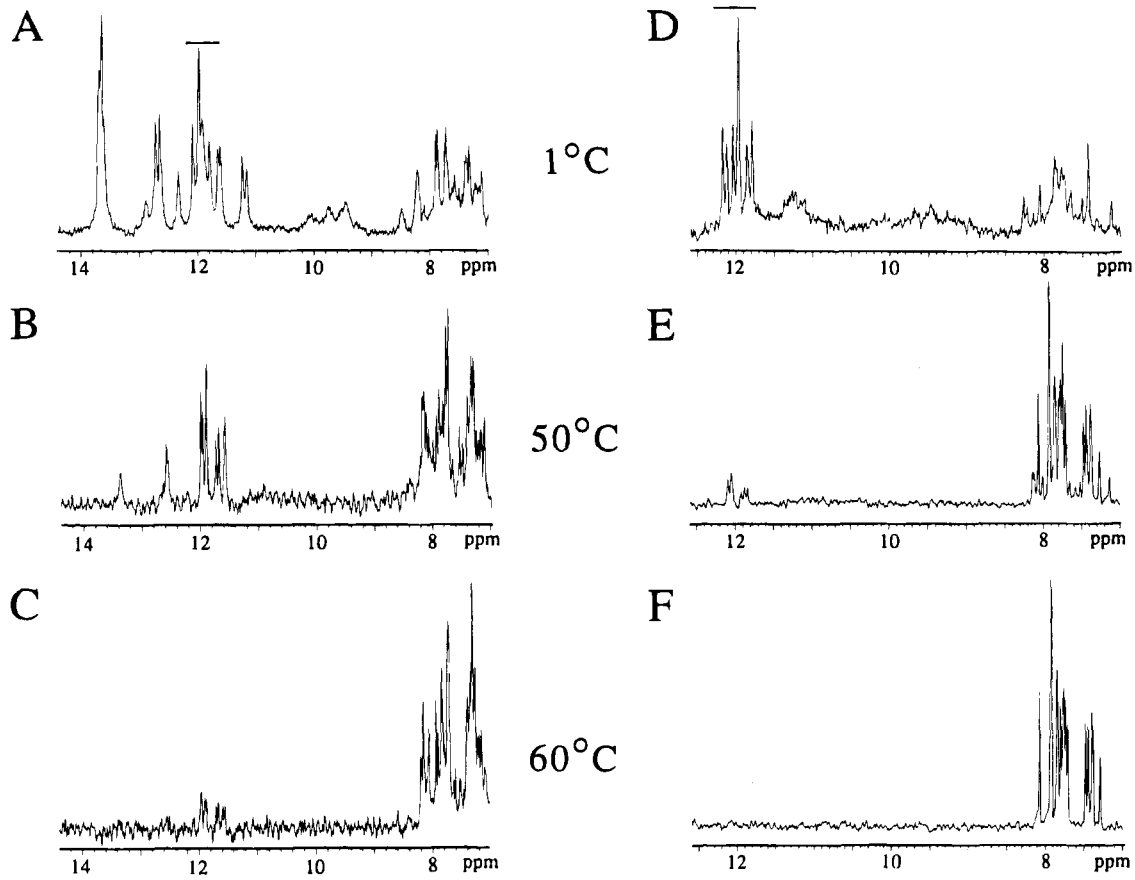

FIGURE 6: One-dimensional ^{1}H NMR spectra of the imino, amino, and aromatic proton resonances of (A−C) oligonucleotide **9** (illustrated in Figure 7A) and (D−F) the 15-mer quadruplex D(GGTTGGTGAGGTTGG) (oligonucleotide **1**) at 1 °C (A, D), 50 °C (B, E), and 60 °C (C, F). The eight G imino resonances corresponding to the quadruplex motif in each molecule are indicated by a solid line above these resonances in the spectra at 1 °C (A, D). Sample conditions were 1.3 mM DNA, 100 mM KCl (A−C) or 2.6 mM DNA, 100 mM KCl (D−F). Both samples were dissolved in 90% H_2O/10% D_2O at pH 6.1. Spectra were acquired and processed as described in Figure 3, with a spectral width of 10 000 Hz and (A) 32, (B) 96, (C) 160, (D) 64, and (E, F) 512 acquisitions.

indicates that such molecules can be optimized by the addition of a conformationally-constrained duplex motif. The demonstration that addition of some duplex sequences, such as that of oligonucleotide **10**, completely offsets the expected higher inhibitory activity of quadruplex/duplex oligonucleotides so that it is only comparable to that of the quadruplex motif alone (oligonucleotide **2**) (Table 2) indicates that the duplex−stem sequence is a strong determinant of inhibitory potency. This is confirmed by inhibition data of two quadruplex/duplex molecules with different 10-base-pair duplex motifs (oligonucleotides **10** and **24**). Although oligonucleotide **24** has a bridged stem motif and oligonucleotide **10** does not, bridging duplex motifs of 8 base pairs or longer do not significantly enhance their thrombin-inhibitory activity as observed for oligonucleotide **8** and the bridged versions of this molecule (oligonucleotides **9** and **22**) (Table 2). This is consistent with the finding that oligonucleotide **8** predominantly forms the unimolecular quadruplex/duplex structure (data not shown). Thus the increased inhibitory potency of oligonucleotide **24** as compared to oligonucleotide **10** (Table 2) is much greater than would be expected from bridging the duplex motif. Also consistent with the importance of the duplex sequence is the finding that three quadruplex/duplex molecules with different 7-base-pair stems (oligonucleotides **19**−**21**) exhibited different inhibitory activity (Table 2).

NMR temperature studies confirmed that the duplex−stem motif is important for the stability of the quadruplex motif. At 1 °C and in the presence of 100 mM KCl, G imino proton resonances corresponding to the quadruplex motif are evident in both the TEG-bridged 32-mer quadruplex/duplex molecule (oligonucleotide **9**) and the 15-mer quadruplex structure (oligonucleotide **1**) (Figure 6A,D). However, at 50 °C the intensity of these imino resonances is much less for the 15-mer than the 32-mer oligonucleotide (Figure 6B,E), and at 60 °C these imino resonances are not present for the quadruplex structure of the 15-mer while they are still evident for the 32-mer (Figure 6C,F). Thus, the melting temperature of the quadruplex motif of oligonucleotide **9** is approximately 60 °C, compared to approximately 50 °C for oligonucleotide **1** under these conditions. The melting temperature of the isolated quadruplex motif (oligonucleotide **2**) has been reported to be 38 °C in the selection buffer and 51 °C in 100 mM KCl (Macaya *et al.*, 1993). The observed stabilization of the quadruplex motif by the duplex stem may be partly responsible for the enhanced potency of the quadruplex/duplex molecules since the inhibition assay was performed in selection buffer at 37 °C, the approximate melting temperature of the isolated quadruplex structure. However, the enhanced potency of quadruplex/duplex molecules is not likely to be due entirely to stabilization of the quadruplex motif by the duplex stem since, as discussed above, several quadruplex/duplex molecules expected to possess comparable stability of their quadruplex motif exhibit significant differences in inhibitory potency. For example, the duplex motif for oligonucleotide **10** shows a UV melting transition (T_m)

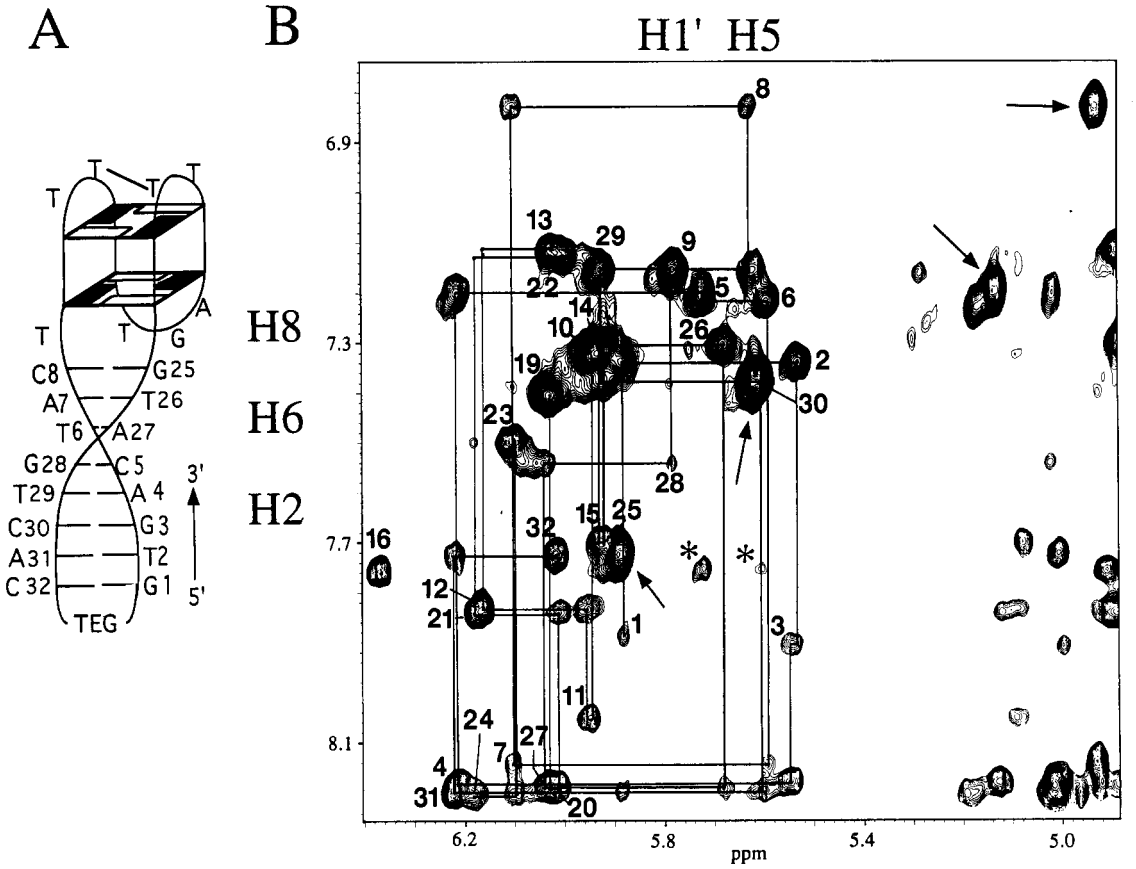

FIGURE 7: (A) Schematic structure of oligonucleotide **9**, a 32-mer circular quadruplex/duplex TEG-bridged oligonucleotide. Rectangles are as in Figure 1. The line between the two T nucleotides represents a T·T base pair. Nucleotides are numbered sequentially starting with G1. (B) Region of NOESY spectrum showing NOE connectivities between base (H_8, H_6, and H_2) and H_1' and $C(H_5)$ protons for the 32-mer quadruplex/duplex oligonucleotide (oligonucleotide **9**) illustrated in panel A. Intranucleotide base (H_8 and H_6) to $H_{1'}$ NOE cross-peaks are numbered according to panel A. Sequential base to $H_{1'}$ connectivities are indicated by solid lines. Intrabase $C(H_6)$–$C(H_5)$ NOE cross-peaks are indicated by arrows. Asterisks (*) indicate an unusual pair of NOEs between the $A4(H_2)$ resonance and the $C5(H_{1'})$ and $C30(H_{1'})$ resonances. Sample was the same as that used for Figure 6A–C except dissolved in 99.996% D_2O. The spectrum was acquired at 25 °C with 2048 complex points, a sweep width of 4600 Hz, a recycle delay of 2 s, a mixing time of 300 ms, 300 t_1 increments, and 64 scans per t_1 increment. The spectrum was zero-filled for a final matrix size of 2048 × 2048 real points and apodized using a shifted Gaussian window function.

at 52 °C, while that of oligonucleotide **8** shows a melting transition at 42 °C (Table 2). These UV melting transitions reflect the melting of the duplex motif since the melting of the quadruplex motif does not give an absorbance change at a 260 nm wavelength. On the basis of this information, one would expect the quadruplex motif of oligonucleotide **10** to be *at least* as stable as that of oligonucleotide **8** and, therefore, expect oligonucleotide **10** to be *at least* as potent of an inhibitor as oligonucleotide **8**. However, oligonucleotide **8** is significantly more potent (Table 2), indicating that stability alone does not determine potency. These results indicate that the duplex motif is a second structural entity which can be optimized and that a more exhaustive search for optimal duplex–stem sequences should yield significantly more potent thrombin inhibitors.

Assignment of Nonexchangeable Proton Resonances of the TEG-Bridged Quadruplex/Duplex (Oligonucleotide 9). Sequence-specific proton resonance assignments for the duplex portion of the structure were determined using standard assignment techniques for double-stranded DNA (Wuthrich, 1986). This was possible because the base (H_8 and H_6) to sugar $H_{1'}$ (Figure 7) and base to $H_{2',2'',3'}$ sequential NOE connectivities (data not shown) are uninterrupted along each chain of the double helix. The I3-U29 derivative containing a deoxyuridine substituted for T29 and a deoxyinosine substituted for G3 served as a resonance marker for the T29-(H_6) and G3(H_8) resonances in the original molecule. These connectivities extended to nucleotide T9 which connects one strand of the double helix to a *syn* guanine in the quadruplex structure. No sequential connectivities were observed between the nucleotides adjacent to the quadruplex motif (T9 and G25) and the first and last nucleotides in the quadruplex (G10 and G24, respectively). It is not surprising that no NOE connectivity was observed between T9 and G10 since the T9 nucleotide is in the *anti* conformation and G10 is in the *syn* conformation, thus giving rise to a *5′-anti-syn-3′* junction, for which such connectivities are not observed (Smith & Feigon, 1992; Macaya *et al.*, 1993). The lack of connectivities between G24 and G25, both in the *anti* conformation, indicates that the helical parameters for the strand from G25 to C32 do not extend to G24 in the quadruplex. The $A(H_2)$ protons were assigned from their NOE cross-peaks to the corresponding Watson–Crick base-paired T imino protons in NOESY spectra in H_2O. Resonance assignments for the bridged but unligated molecule, containing a 5′–3′ "nick" between nucleotides G28 and T29 (oligonucleotide **7**) (numbering as in Figure 7A), were very similar and served as confirmation for the assignments of the circular ligated molecule (oligonucleotide **9**). The base to sugar sequential connectivities were not interrupted at the

Table 3: ^{1}H NMR Resonance Assignments for Oligonucleotide **9** at 25 °C[a]

residue	H_8, H_6	methyl, H_5, H_2	$H_{1'}$	$H_{2'}$	$H_{2''}$	$H_{3'}$	$H_{4'}$	imino[b]	amino[b]
G1	7.89		5.88	2.75	3.77	4.82		12.89	
T2	7.34	1.59	5.53	2.12	2.38	4.78	4.14	13.69	
G3	7.91		5.55	2.69	2.76	4.99	4.35	12.65	
A4	8.18	7.69	6.21	2.65	2.87	5.01			
C5	7.2	5.13	5.72	1.84	2.38	4.64	4.14		7.92, 6.67
T6	7.22	1.48	5.59	2	2.35	4.79		13.6	
A7	8.14	8.29	6.1	2.55	2.76	4.93			
C8	6.83	4.93	5.63	1.45	2.23	4.51	4.02		7.54, 6.50
T9	7.16	1.21	5.78	2.23	2.42	4.83			
G10	7.34		5.95	3.51	2.85	4.8		11.6	
G11	8.05		5.95	2.91	2.28	5.09	4.33	11.91	
T12	7.83	1.94	6.16	2.15	2.52	4.86	4.26		
T13	7.13	0.96	5.99	2.01	2.58	4.83		11.16	
G14	7.31		5.92	3.34	2.8	4.82		11.98	
G15	7.7		5.92	2.67	2.47	5.08	4.38	11.78	10.05, 6.57
T16	7.76	1.94	6.37	2.47	2.57	4.91	4.33		
G17								9.75	4.49, 4.49
A18									
G19	7.41		6.02	3.62	2.88	4.92		11.65	9.46, 6.86
G20	8.19		6.01	2.99	2.32	5.12	4.38	11.98	
T21	7.84	1.95	6.17	2.2	2.55	4.9	4.27		
T22	7.12	1	6.02	2.05	2.62	4.89		11.24	
G23	7.5		6.1	3.65	3.08	4.96	4.41	12.07	9.47, 6.81
G24	8.2		6.18	2.82	2.7	5.19	4.45	11.88	
G25	7.7		5.92	2.54	2.65	4.79		12.33	
T26	7.31	1.23	5.68	2.11	2.43	4.88	4.2	13.65	
A27	8.19	7.12	6.04	2.75	2.88	5.02	4.39		7.58, 7.31
G28	7.54		5.78	2.43	2.66	4.83		12.72	
T29	7.17	1.2	5.93	2.02	2.42	4.79		13.63	
C30	7.38	5.62	5.6	1.83	2.27	4.8	4.07		8.48, 6.98
A31	8.2	7.88	6.22	2.66	2.66	5.01			
C32	7.73	5.89	6.01	2.23	2.42	4.74			7.60, 6.40

[a] Numbering as shown in Figure 7A. [b] Chemical shifts obtained from NOESY spectrum in H_2O at 1 °C.

5′−3′ "nick", indicating that the presence of a "nick" does not disrupt the stacking or helical parameters at that junction (data not shown).

The sequence-specific assignment of the quadruplex resonances required the comparison of NOESY spectra of the two molecules with deoxyinosine substitutions in the quadruplex motif with spectra of the original molecule. This was necessary due to interruptions in sequential connectivities at 5′-*anti-syn*-3′ steps and in the TGA loop after nucleotides T13, G15, T16, A18, T22, and G24. The deoxyinosine H_8 proton is easily distinguished from the other guanine H_8 protons due to its downfield shift and therefore serves as a resonance marker in the fragmented sequential connectivities of the quadruplex. The I11 deoxyinsoine derivative allowed for the distinction between the G10-G11-T12-T13 and G19-G20-T21-T22 base to sugar sequential connectivities. The I24 deoxyinosine derivative allowed for the distinction between the G23-G24 and G14-G15 base to sugar connectivities. All $H_{1'}$, $H_{2'}$, $H_{2''}$, and $H_{3'}$ assignments were confirmed for each deoxyribose ring from intraresidue connectivities between these proton resonances in a HOHAHA spectrum. These assignments were extended to the $H_{4'}$ resonances when possible using the connectivities from the HOHAHA spectrum. The $H_{5'}$ and $H_{5''}$ resonances were not assigned due to severe spectral overlap in this region. The deoxyinosine derivatives were also used to determine the quartet structures (*i.e.*, which guanine bases are H-bonded to each other) by observation of NOE cross-peaks between inosine H_2 protons, which have a characteristic low-field chemical shift, and the H_8 proton from the guanine base to which it is H-bonded. Such NOEs were observed between I11(H_2) and G23(H_8) and between I24(H_2) and G10(H_8). The quartet structures were determined unambiguously from these two cross-peaks, the fact that the structure is unimolecular, and the requirement that G10 and G24 must be at the quadruplex−duplex junction. This approach of using deoxyinosine-substituted oligonucleotides has been used to determine the base-pairing partners and resonance assignments for other DNA quadruplexes (Smith & Feigon, 1992; Macaya *et al.*, 1993; Schultze *et al.*, 1994). The chemical shift assignments for the nonexchangeable protons are listed in Table 3.

Assignment of Exchangeable Proton Resonances of Oligonucleotide ***9***. The imino proton resonances in the duplex portion of the structure were assigned from the imino−imino connectivities between adjacent base pairs from NOESY spectra in H_2O (Figure 8). Assignments were then extended to the C amino and, when possible, A amino protons from imino−amino NOE cross-peaks within each Watson−Crick base pair. The sequence-specific G imino and C amino assignments were confirmed by intrabase NOE cross-peaks between C amino protons and previously-assigned C(H_5) protons. The I3-U29 deoxyinosine and deoxyuridine derivative was also used as a resonance marker for the imino−imino connectivities. The similarity in the imino chemical shifts from the unligated molecule (oligonucleotide **7**) confirmed the resonance assignments. The imino−imino connectivities were not interrupted at the 5′−3′ "nick" in this unligated molecule, indicating once again that the nucleotide base pairs are stacked at the "nick" in the duplex structure (data not shown).

The inosine-substituted derivatives were used to assign the imino protons in the quadruplex structure since the large downfield shift of the inosine imino resonances served as

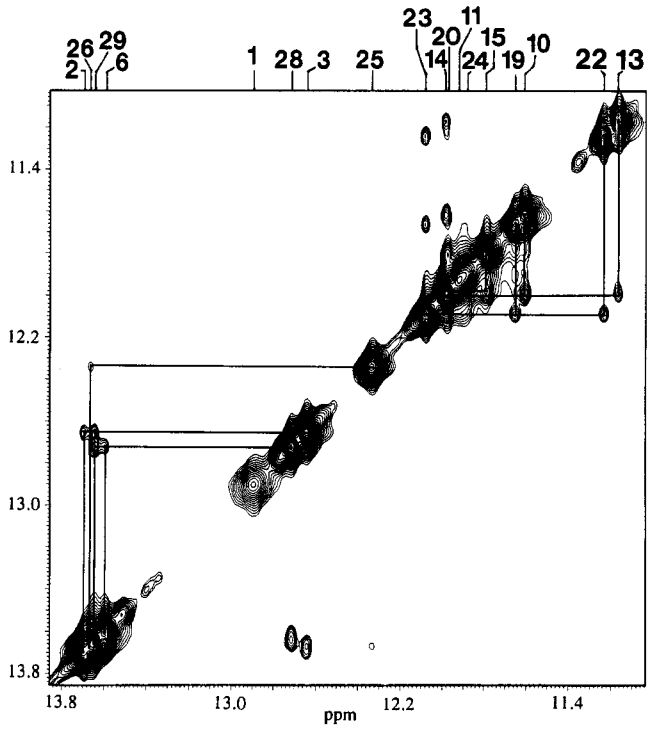

FIGURE 8: Region of imino−imino NOE connectivities between H-bonded imino protons in oligonucleotide **9** for the same sample as in Figure 6A−C (illustrated in 7A). NOE connectivities between adjacent Watson−Crick base pairs along the duplex−stem motif are indicated by connecting lines above the diagonal; NOE connectivities between stacked guanine bases within the two G quartets and between the T iminos from the stacked T·T base pair and the G iminos from the top G quartet are indicated by connecting lines below the diagonal. Assignments for these imino proton resonances are indicated on the top of the spectrum, using the numbering scheme from Figure 7A. The SS NOESY was acquired at 1 °C in 90% H_2O/10% D_2O, with a 208 μs SS pulse (Smallcombe, 1993), 2048 complex points, a relaxation delay of 1.9 s, a mixing time of 100 ms, a sweep width of 10 000 Hz, 400 t_1 increments, and 128 scans per t_1 value. The spectrum was processed by linear predicting the first two data points of the FID, zero-filling for a final matrix size of 2048 × 2048 real points, and solvent subtracting the residual water peak and apodized using a shifted Gaussian window function.

resonance markers. The four G imino protons corresponding to the lower quartet (G10, G15, G19, and G24) were identified, but not assigned sequence-specifically, from NOE cross-peaks between the G17 amino protons in the TGA loop and all four G iminos from this bottom quartet (Figure 9). Such NOEs are only possible if all corresponding G iminos are in the same quartet, adjacent to the TGA loop. The I11 and I24 deoxyinosine derivatives allowed for the assignment of the G11 and G24 iminos. The G14 and G23 imino protons were assigned from their NOE cross-peaks to T13-($H_{2'2''}$) and T22($H_{2'2''}$) protons, respectively. The T13 and T22 iminos were assigned from NOEs to G14 and G23, respectively. NOEs between the T13 imino proton and the imino protons of both G14 and G11 confirmed the assignment of G11 since the G14 imino was already identified. In an analogous way, the G20 imino proton was assigned from NOE cross-peaks between the T22 imino and both the G20 and G23 iminos. Once all the G iminos in the top quartet were assigned, all the G iminos in the bottom quartet were sequence-specifically assigned from NOEs between G iminos in the bottom quartet and G iminos which are stacked above them in the top quartet (*i.e.*, imino−imino NOEs between G11 and G24, G19 and G23, G15 and G20, and G14 and G10) (Figure 8). Resolved G amino protons were assigned from intrabase imino−amino NOEs. All the above assignments require the knowledge of the base-pairing partners in each G quartet which was determined from the deoxyinosine-substituted derivatives. All of these NOE connectivities and assignments are analogous to those obtained from a previous NMR study of the 15-mer oligonucleotide d(GGTTGGTGTGGTTGG) which consisted of only the quadruplex structure (Macaya *et al.*, 1993; Schultze *et al.*, 1994). The resonance assignments of the exchangeable protons are listed in Table 3.

Structure of the TEG-Bridged Quadruplex/Duplex Oligonucleotide ***9****. (1) Duplex Structural Characteristics.* All eight Watson−Crick base pairs in the duplex−stem were evident from the sequential imino−imino NOE cross-peaks. Only the G imino proton resonance adjacent to the TEG bridge lacked an imino−imino NOE to the adjacent base pair (Figure 8), indicating that it was in faster exchange with solvent. This increased exchange rate for the terminal imino proton could be due to a slight "buckling" or distortion of the last base pair in order to accommodate the TEG bridge. A longer bridge, such as a tetraethylene glycol, would be expected to be less distorting to the terminal base pair. The presence of uninterrupted sequential base−sugar connectivities indicates that the helix is not disrupted at any point since no discontinuity is observed. NOE cross-peaks between C(H_5) (Figure 7B) and T(methyl) (data not shown) protons and base protons (H_8 or H_6) from the 5′ base indicate that the helix is right-handed (Wuthrich, 1986). Some unexpected NOE cross-peaks in the region of base to $H_{1'}$ and C(H_5) NOEs were pairs of cross-peaks between A(H_2) protons and the H1′ protons from the 3′ nucleotide on the same strand and the 3′ nucleotide on the complementary strand. For example, the A4(H_2) proton has a cross-peak to both the C5($H_{1'}$) and C30($H_{1'}$) protons (Figure 7B). These NOE pairs, which are analogous to those found in RNA helices between G amino protons [instead of A(H_2)] and the two respective $H_{1'}$ protons, have been used as a marker for A-type helices (Heus & Pardi, 1991). These unusual NOE cross-peaks are also observed in NOESY spectra of the unbridged molecule (oligonucleotide **8**) (data not shown). Therefore, these cross-peaks are not due to helical distortions caused by the presence of a bridge at the end of the helix. Preliminary data indicates the sugar conformations in the duplex motif are S-type (data not shown). However, whether or not the structural features of the duplex motif are consistent with an A-type or B-type helix requires further investigation. It is possible that the T9 base, which is not base-paired and is at the junction of the quadruplex and duplex motifs, is folded away from the quadruplex motif into the minor groove of the duplex. The low-field chemical shift of A7(H_2) (Table 3) could be the result of a ring current effect if the T9 base is folded into the minor groove such that the A7(H_2) proton is in the plane of the T9 base.

(2) Quadruplex Structural Characteristics. The pattern of glycosidic torsion angles alternates 5′-G_{syn}-G_{anti}-3′ along each strand of the quadruplex, and the glycosidic torsion angles in the two quartets are $G10_{syn}$−$G15_{anti}$−$G19_{syn}$−$G24_{anti}$ and $G11_{anti}$−$G14_{syn}$−$G20_{anti}$−$G23_{syn}$ (numbering as in Figure 7A). Such observations indicated that the structure of the quadruplex motif is topologically the same in this quadruplex/duplex structure as was found in the isolated

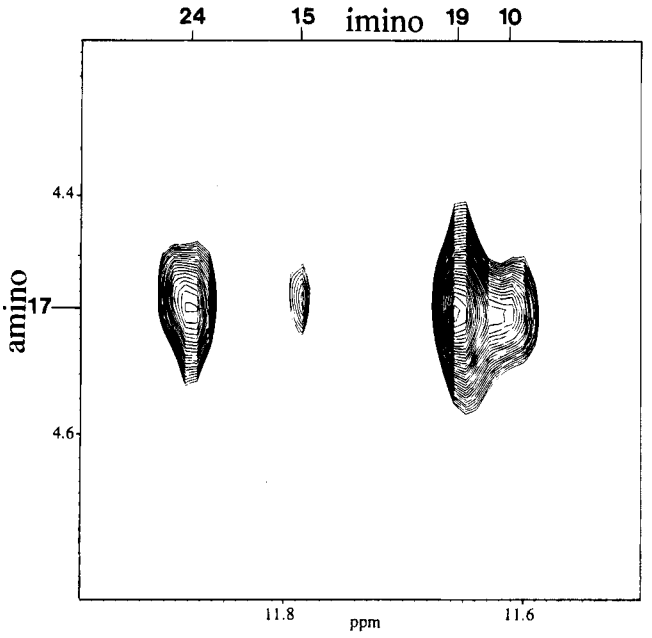

FIGURE 9: Region of NOE cross-peaks between the G17 (in the TGA loop) amino protons and all four G imino protons from the bottom G quartet of oligonucleotide **9** as illustrated in Figure 7A. The G17 amino resonances (both at the same chemical shift) are assigned on the left of the spectrum, and the four G imino resonances are assigned on top of the spectrum according to the numbering scheme in 7A. The sample and spectrum are the same as were used in Figure 8.

quadruplex motif (Macaya *et al.*, 1993; Schultze *et al.*, 1994; Wang *et al.*, 1993a); *i.e.*, there are two narrow grooves spanned by the two T−T loops above the top quartet and two wide grooves, one of which is spanned by the TGA loop (the other wide groove being part of quadruplex−duplex junction). The presence of imino−imino NOEs between T13 and G14 and between T22 and G23 indicate that these T imino protons are in slow exchange with solvent, which is consistent with T13 and T22 forming a previously-proposed T·T base pair between the T−T loops in this structure (Macaya *et al.*, 1993; Schultze *et al.*, 1994). The other two T iminos in these loops are not observed due to their fast exchange rate, indicating they are not H-bonded.

The conformation of the T16-G17-A18 loop spanning one of the wide grooves has some similarities to that determined for the TGT loop spanning the same groove in the thrombin-binding quadruplex d(GGTTGGTGTGGTTGG). T16 from the quadruplex/duplex molecule does not show any sequential NOE connectivities (Figure 7B), and its chemical shifts (Table 3) are very similar to those corresponding to the first T in the TGT loop of the referenced quadruplex motif (Schultze *et al.*, 1994). These results are consistent with this T nucleotide being folded sideways into the wide groove that this loop spans as previously observed (Macaya *et al.*, 1993; Schultze *et al.*, 1994; Wang *et al.*, 1993a). The G17 base is stacked under the bottom quartet as evidenced by an imino−imino NOE cross-peak between nucleotides G17 and G10 (not shown) and the NOE cross-peaks between the G17 amino protons and all four G iminos from the adjacent quartet (Figure 9). The presence of these NOE cross-peaks and the lack of NOEs between the quadruplex and duplex motifs indicate that the G17 base in the TGA loop is most likely stacked between the quadruplex and duplex motifs. The unusually high-field chemical shifts of the H_5, H_6, and $H_{2'}$ resonances of C8 (Table 3), the last nucleotide on one duplex helix adjacent to the quadruplex motif, are evidence that the G17 base is likely to be stacked above C8, thereby inducing such ring current shifts. It is likely that A18 is also stacked under the bottom quartet, as reported for the second T base of the TGT loop (Macaya *et al.*, 1993; Wang *et al.*, 1993a; Schultze *et al.*, 1994), but the lack of assignments for this base did not allow this to be determined.

Although the quadruplex motif characterized in this NMR study contains a TGA loop, quadruplex structures with a TGT loop are more inhibitory to thrombin activity (Table 2). This finding is consistent with reports that the quadruplex molecules which bind most tightly to thrombin have the consensus sequence TNT (where N is variable) in this loop (Wang *et al.*, 1993b). The fact that the T16 base is folded into the wide groove away from the remaining part of the loop indicates that the G17−A18 sequence does not require T16 to span the wide groove. The GA sequence may be uniquely suited to do this since only this sequence has been selected for 2-base loops spanning the wide groove of the quadruplex in this selection (Figure 1A) and the previously reported selection (Bock *et al.*, 1992).

Serum Stability. Bridging of the 5′ and 3′ ends of the oligonucleotides studied raised the possibility that these molecules might show enhanced resistance nuclease degradation in serum. To investigate this possibility, an ion-exchange HPLC method was employed (see Materials and Methods). Evaluation of the unbridged 15-mer quadruplex (oligonucleotide **1**) indicated that it was rapidly degraded with a half-life of approximately 17 min, which is consistent with data reported for other natural DNA oligonucleotides (Akhtar *et al.*, 1991), in which the primary route of degradation has been shown to be due to cleavage by 3′-exonucleases (Shaw *et al.*, 1991). The disulfide-bridged quadruplex (oligonucleotide **13**) was much more stable, with a half-life of nearly 6 h under the same conditions. TEG- or disulfide-bridged molecules with 8-base-pair stems (oligonucleotides **9** and **22**, respectively) were even more stable, with half-lives of approximately 12 and 10 h, respectively. This represents increases of 42-fold (oligonucleotide **9**) and 35-fold (oligonucleotide **22**), respectively, over that of the unmodified 15-mer (oligonucleotide **1**) (Figure 10). The increase in stability is consistent with a reduction in the sensitivity to 3′-exonucleases due to bridging the 3′ and 5′ ends of the duplex motif.

Inhibitory Activity of Bridged and Unbridged Molecules in Serum. To test the inhibitory activity of bridged (oligonucleotides **9** and **16**) and unbridged (oligonucleotide **1**) molecules in human serum, an alternative clotting reaction was performed in which oligonucleotides were preincubated in serum for 1 h prior to the clotting assay (see Materials and Methods). In the absence of DNA, the clotting reaction was faster in the presence of serum than in the presence of the selection buffer (Table 4). This indicates that factors in serum allow the clotting reaction to proceed more efficiently. Bridged oligonucleotides **9** and **16** significantly extended the clotting time compared to that for the uninhibited reaction, even when these oligonucleotides were preincubated in serum for 1 h (Table 4). In contrast, the unbridged 15-mer quadruplex (oligonucleotide **1**) lost almost all inhibitory activity after incubation in serum. These results correlated with the data from serum stability studies presented above in that the bridged molecules with longer half-lives retain

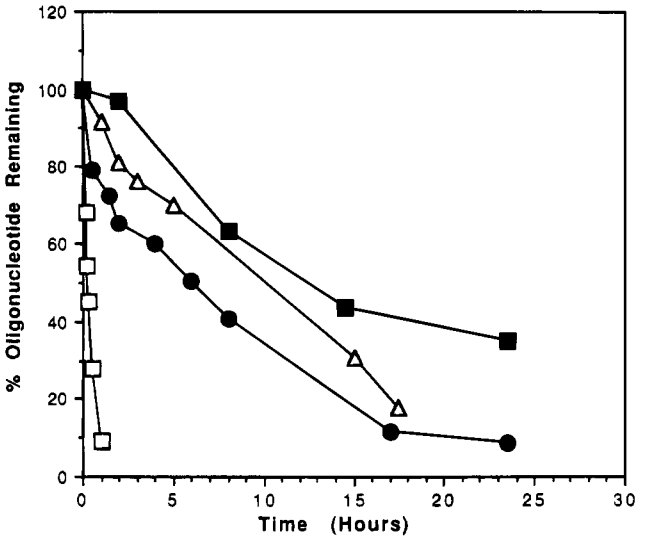

FIGURE 10: Plot of percent oligonucleotide remaining versus incubation time (h) in human serum pooled from three individuals for bridged molecules [oligonucleotides **9** (■), **13** (●), and **22** (△)] and unbridged molecules [oligonucleotide **1** (□)].

Table 4: Inhibitory Activity of Oligonucleotides after Exposure to Serum[a]

oligonucleotide	incubation[b]	clotting time (s)
none	selection buffer	56
none	human serum	45
9	selection buffer	488
9	human serum	326
16	selection buffer	362
16	human serum	218
1	selection buffer	151
1	human serum	50

[a] Final concentrations were 9.7 nM thrombin and 50 nM DNA. [b] Oligonucleotides were incubated in human serum or selection buffer for 1 h prior to the clotting reaction.

higher inhibitory activities than the more labile unbridged molecules. The enhanced inhibition of clot formation together with substantially longer half-lives in serum suggests that bridged quadruplex/duplex molecules may be attractive candidates for development as antithrombotic agents.

CONCLUSIONS

A series of novel quadruplex/duplex DNA structures have been selected on the basis of their affinity for thrombin. These molecules were shown to inhibit thrombin, and this inhibition was improved using a rational approach, suggested by results of structural NMR studies, in which the lead molecules were constrained to a biologically active conformation. This approach, which involved bridging the 5′−3′ ends of duplex structures, may prove relevant for the optimization of oligonucleotides which bind to other clinically important targets. The resistance to nucleases and the greater activity of bridged quadruplex/duplex structures make them attractive candidates for their development as antithrombotics. It is interesting to note that an analogous approach in which a hirudin peptide fragment was conformationally restricted through cyclization also resulted in a more potent thrombin inhibitor with increased metabolic stability (Szewczuk *et al.*, 1992). We have demonstrated that both the length and sequence of the duplex−stem are important determinants for the potency of thrombin inhibition. Since we have not undertaken an exhaustive search for optimal duplex−stem sequences, it is likely that such an effort would yield even more potent thrombin inhibitors.

ACKNOWLEDGMENT

We thank Dr. Michael I. Sherman and Dr. Paul P. Trotta for critical review of the manuscript and Kenneth Nawoschik for synthesis and purification of oligonucleotides.

REFERENCES

Akhtar, S., Kole, R., & Juliano, R. L. (1991) *Life Sci. 49*, 1793−1801.
Bax, A., & Davis, D. G. (1985) *J. Magn. Reson. 65*, 355−360.
Blommers, M. J. J., Walters, J. A. L. I., Haasnoot, C. A. G., Aelen, J. M. A., van der Marel, G. A., van Boom, J. H., & Hilbers, C. W. (1989) *Biochemistry 28*, 7491−7498.
Bock, L. C., Griffin, L. C., Latham, J. A., Vermaas, E. H., & Toole, J. J. (1992) *Nature 355*, 564−566.
Boulard, Y., Gabarro-Arpa, J., Cognet, J. A. H., Le Bret, M., Guy, A., Teoule, R., Guschlbauer, W., & Fazakerley, G. V. (1991) *Nucleic Acids Res. 19*, 5159−5167.
Davis, D. G., & Bax, A. (1985) *J. Am. Chem. Soc. 107*, 2820−2821.
Ellington, A. D., & Szostak, J. W. (1990) *Nature 346*, 818−822.
Ellington, A. D., & Szostak, J. W. (1992) *Nature 355*, 850−852.
Gao, H., Chidambaram, N., Chen, B. C., Pelham, D. E., Patel, R., Yang, M., Zhou, L., Cook, A. F., & Cohen, J. S. (1994) *Bioconj. Chem. 5*, 445−453.
Gao, H., Yang, M., & Cook, A. F. (1995) *Nucleic Acids Res. 23*, 285−292.
Glick, G. D. (1991) *J. Org. Chem. 56*, 6746−6747.
Glick, G. D., Osborne, S. E., Knitt, D. S., & Marino, J. P. (1992) *J. Am. Chem. Soc. 114*, 5447−5448.
Griffin, L. C., Tidmarsh, G. F., Bock, L. C., Toole, J. J., & Leung, L. L. K. (1993) *Blood 81*, 3271−3276.
Gupta, G., Garcia, A. E., & Hiriyanna, K. T. (1993) *Biochemistry 32*, 948−960.
Heus, H. A., & Pardi, A. (1991) *J. Am. Chem. Soc. 113*, 4360−4361.
Jellinek, D., Lynott, C. K., Rifkin, D. B., & Janjic, N. (1993) *Proc. Natl. Acad. Sci. U.S.A. 90*, 11227−11231.
Jenison, R. D., Gill, S. C., Pardi, A., & Polisky, B. (1994) *Science 263*, 1425−1429.
Kallick, D. A., & Wemmer, D. E. (1991) *Nucleic Acids Res. 19*, 6041−6046.
Kinzler, K. W., & Vogelstein, B. (1989) *Nucleic Acids Res. 17*, 3645−3653.
Kubik, M. F., Stephens, A. W., Schneider, D., Marlar, R. A., & Tasset, D. (1994) *Nucleic Acids Res. 22*, 2619−2626.
Kumar, A., Ernst, R. R., & Wuthrich, K. (1980) *Biochem. Biophys. Res. Commun. 95*, 1−6.
Levitt, M. H., Freeman, R., & Frenkiel, T. (1982) *J. Magn. Reson. 47*, 328−330.
Macaya, R. F., Schultze, P., Smith, F. W., Roe, J. A., & Feigon, J. (1993) *Proc. Natl. Acad. Sci. U.S.A. 90*, 3745−3749.
Marion, D., & Bax, A. (1988) *J. Magn. Reson. 80*, 528−533.
Ng, A. S., Lewis, S. D., & Shafer, J. A. (1993) *Methods Enzymol. 222*, 341−358.
Oliphant, A. R., Brandl, C. J., & Struhl, K. (1989) *Mol. Cell. Biol. 9*, 2944−2949.
Orbons, L. P. M., van der Marel, G. A., van Boom, J. H., & Altona, C. (1987) *Eur. J. Biochem. 170*, 225−239.
Paborsky, L. R., McCurdy, S. N., Griffin, L. C., Toole, J. J., & Leung, L. L. K. (1993) *J. Biol. Chem. 268*, 20808−20811.
Padmanabhan, K., Padmanabhan, K. P., Ferrara, J. D., Sadler, J. E., & Tulinsky, A. (1993) *J. Biol. Chem. 268*, 17651−17654.
Pei, D., Ulrich, H. D., & Schultz, P. G. (1991) *Science 253*, 1408−1411.
Schultze, P., Macaya, R. F., & Feigon, J. (1994) *J. Mol. Biol. 235*, 1532−1547.

Shaw, J.-P., Kent, K., Bird, J., Fishback, J., & Froehler, B. (1991) *Nucleic Acids Res. 19*, 747−750.

Sherman, M. I., Bertelsen, A. H., & Cook, A. F. (1993) *Bioorg. Med. Chem. Lett. 3*, 469−475.

Smallcombe, S. H. (1993) *J. Am. Chem. Soc. 115*, 4776−4785.

Smith, F. W., & Feigon, J. (1992) *Nature 356*, 164−168.

States, D. J., Haberkorn, R. A., & Ruben, D. J. (1982) *J. Magn. Reson. 48*, 286−292.

Szewczuk, Z., Gibbs, B. F., Yue, S. Y., Purisima, E. O., & Konishi, Y. (1992) *Biochemistry 31*, 9132−9140.

Tuerk, C., & Gold, L. (1990) *Science 249*, 505−510.

Tuerk, C., MacDougal, S., & Gold, L. (1992) *Proc. Natl. Acad. Sci. U.S.A. 89*, 6988−6992.

Wang, K. Y., McCurdy, S., Shea, R. G., Swaminathan, S., & Bolton, P. H. (1993a) *Biochemistry 32*, 1899−1904.

Wang, K. Y., Krawczyk, S. H., Bischofberger, N., Swaminathan, S., & Bolton, P. H. (1993b) *Biochemistry 32*, 11285−11292.

Wu, Q., Tsiang, M., & Sadler, J. E. (1992) *J. Biol. Chem. 267*, 24408−24412.

Wuthrich, K. (1986) *NMR of Proteins and Nucleic Acids*, John Wiley & Sons, New York, NY.

BI942554I